JCB Article

Abelson kinase regulates epithelial morphogenesis in *Drosophila*

Elizabeth E. Grevengoed,[1] Joseph J. Loureiro,[2] Traci L. Jesse,[3] and Mark Peifer[1,2,3]

[1]Curriculum in Genetics and Molecular Biology, [2]Department of Biology, and [3]Lineberger Comprehensive Cancer Center, University of North Carolina at Chapel Hill, Chapel Hill, NC 27599

Activation of the nonreceptor tyrosine kinase Abelson (Abl) contributes to the development of leukemia, but the complex roles of Abl in normal development are not fully understood. *Drosophila* Abl links neural axon guidance receptors to the cytoskeleton. Here we report a novel role for *Drosophila* Abl in epithelial cells, where it is critical for morphogenesis. Embryos completely lacking both maternal and zygotic Abl die with defects in several morphogenetic processes requiring cell shape changes and cell migration. We describe the cellular defects that underlie these problems, focusing on dorsal closure as an example. Further, we show that the Abl target Enabled (Ena), a modulator of actin dynamics, is involved with Abl in morphogenesis. We find that Ena localizes to adherens junctions of most epithelial cells, and that it genetically interacts with the adherens junction protein Armadillo (Arm) during morphogenesis. The defects of *abl* mutants are strongly enhanced by heterozygosity for *shotgun*, which encodes DE-cadherin. Finally, loss of Abl reduces Arm and α-catenin accumulation in adherens junctions, while having little or no effect on other components of the cytoskeleton or cell polarity machinery. We discuss possible models for Abl function during epithelial morphogenesis in light of these data.

Introduction

The nonreceptor tyrosine-kinase Abl is the cellular homologue of *v-abl*, the transforming gene of Abelson (Abl)* murine leukemia virus (for review see Zou and Calame, 1999; Mauro and Druker, 2001). Bcr-Abl, an activated, chimeric form of Abl resulting from a chromosomal translocation, plays a causative role in human chronic myelogenous and acute lymphocytic leukemia. Bcr-Abl has deregulated tyrosine kinase activity, and an inhibitor of this kinase has shown promise in treating leukemia. Multiple substrates for oncogenic Abl kinase in diverse signaling pathways have been identified, revealing complex effects of Abl misregulation.

Abl's normal role has remained more elusive. Abl homologues are found in all animals. All share conserved NH_2-terminal SH3, SH2, and tyrosine kinase domains, as well as distinct COOH-terminal F- and G-actin binding domains (for review see Lanier and Gertler, 2000). Mammalian Abl, unlike its fly homologue, also contains nuclear import and export signals and a COOH-terminal DNA binding domain, and thus it localizes to both nuclei and the cytoplasm. In nuclei, it is thought to regulate the cell cycle and the response to DNA damage (for review see Van Etten, 1999). Cytoplasmic Abl predominantly associates with the actin cytoskeleton (e.g., van Etten et al., 1994) and can be found at cell–matrix junctions in cultured cells (Lewis et al., 1996). The different subcellular pools of Abl may perform distinct functions, though Abl can translocate to nuclei in response to cytoplasmic cues (Lewis et al., 1996). Bcr-Abl exclusively localizes to the cytoplasm, suggesting that its role in oncogenesis involves cytoplasmic targets.

In *Drosophila*, Abl localizes to the axons of the central nervous system (CNS) (Bennett and Hoffmann, 1992). In epithelial cells, Abl's localization varies with stage of development and tissue, but it is often concentrated near the apical cortex. Abl localizes to apical cell junctions soon after cells form and to the apical cytoplasm during gastrulation and in imaginal discs. In contrast, it is diffusely cytoplasmic in extended germband embryos.

Genetic analyses in mice and flies have begun to shed light on Abl's biological function. *abl* mutant mice are embryonic-viable but runted and exhibit defects in develop-

The online version of this paper contains supplemental material.

Address correspondence to Mark Peifer, CB#3280, Department of Biology, Coker Hall, University of North Carolina at Chapel Hill, Chapel Hill, NC 27599-3280. Tel.: (919) 962-2271. Fax: (919) 962-1625. E-mail:peifer@unc.edu

Elizabeth E. Grevengoed and Joseph J. Loureiro contributed equally to this paper.

*Abbreviations used in this paper: Abl, Abelson; abl^{MZ}, *abl* maternal/zygotic; Arm, Armadillo; CNS, central nervous system; dab, disabled; Ena, Enabled; GFP, green fluorescent protein; scb, scab; shg, shotgun.

Key words: Abelson kinase; Armadillo; adherens junctions; enabled; *Drosophila*

ment of the bones, immune system, and sperm. A null mutation and a COOH-terminal truncation removing the actin binding domains have similar phenotypes, suggesting that the interaction with actin is functionally important (for review see Van Etten, 1999). Analysis of Abl function in mice is complicated by the presence of the related kinase Arg; mice lacking both *abl* and *arg* die as embryos with defects in neurulation that may reflect problems in actin organization (Koleske et al., 1998).

In *Drosophila*, analysis of the single Abl homologue primarily revealed roles in neural development. *abl* mutants are pupal lethal with defects in retinal development (Henkemeyer et al., 1987); they also have subtle CNS defects in which certain axons stop short of innervating their target muscles (Wills et al., 1999b). Much more severe CNS defects are seen in *abl* mutants that are also heterozygous or homozygous for the neural cell adhesion molecule *fasciclin*, the receptor tyrosine phosphatase *dLAR*, the axon guidance receptor *robo,* the adaptor *disabled (dab)*, the Rho-family GEF *trio*, or the actin regulator *profilin* (for review see Lanier and Gertler, 2000). These data led to a model in which Abl transduces signals from neural cell surface receptors, influencing actin dynamics in growth cones.

In doing so, Abl is thought to act via one of its substrates, Enabled (Ena; Comer et al., 1998). Originally identified as a suppressor of *abl; dab/+* mutants (Gertler et al., 1990), Ena is a member of the Ena/VASP family (for review see Lanier and Gertler, 2000), which modulate actin dynamics (Gertler et al., 1996). *Drosophila ena* mutants are embryonic lethal with defects in the CNS and its peripheral projections (Gertler et al., 1990; Wills et al., 1999a). The effects of *ena* mutations are opposite to those of *abl;* axons go past their muscle targets rather than stopping short, consistent with the idea that Abl negatively regulates Ena. Like Abl, Ena is thought to act downstream of the axon guidance receptors Robo (Bashaw et al., 2000) and dLAR (Wills et al., 1999a), mediating cytoskeletal events.

Our interest in *abl* emerged from its genetic interactions with the adherens junction protein Armadillo (Arm; Loureiro and Peifer, 1998). We investigate morphogenesis, the process by which animals create their complex body plans by organized cell shape changes and rearrangements. Epithelial cells must remain in intimate contact throughout morphogenesis, and in order to change shape or move must coordinate their actin cytoskeletons. Cells accomplish these tasks via cell–cell adherens junctions, which form a continuous adhesive belt around the apex of each cell that anchors a contractile ring of actin filaments (for review see Tepass et al., 2000). Junctions are organized around transmembrane cadherins. Human E-cadherin mediates cell–cell adhesion and organizes a multiprotein complex of catenins bound to its cytoplasmic tail, binding directly to β-catenin, which in turn anchors actin via interactions with α-catenin. *Drosophila* E-cadherin, Arm (the β-catenin homologue), and α-catenin function similarly.

Cadherin-catenin–mediated adhesion must be dynamic, allowing cell movement during morphogenesis (for review see Tepass et al., 2000). We used a genetic approach in *Drosophila* to identify regulators of epithelial morphogenesis. *abl* mutations substantially enhance the CNS defects of *arm* mutants. Further, *abl* genetically interacts with *arm* in the epidermis (Loureiro and Peifer, 1998). This suggested that Abl acts in epidermal cells during morphogenesis. Thus, we investigated whether Abl regulates epithelial development in *Drosophila*. Previous studies of Abl function relied on zygotic mutations, and thus the maternal contribution of Abl may have masked roles in other developmental processes. We removed this maternal contribution, analyzing *abl* maternal/zygotic mutants. This revealed a requirement for Abl in epithelial morphogenesis. Here we report the characterization of this role.

Results

Abelson is essential for embryonic morphogenesis

Previous studies identified a role for Abl in the CNS. Zygotic *abl* mutants have subtle CNS defects, that are enhanced in double mutant combinations (for review see Lanier and Gertler, 2000). We found previously that *abl* interacts with *arm* in its role as a catenin during CNS development (Loureiro and Peifer, 1998), where Arm works with N-cadherin (Iwai et al., 1997). We also observed genetic interactions between *abl* and *arm* in the epidermis. Thus, we hypothesized that Abl might also act in epithelial cells, and that this role might be masked by maternally contributed Abl. To test this, we removed maternal and zygotic Abl using the FLP dominant female sterile technique (Chou and Perrimon, 1996) to generate *abl* heterozygous females whose germ lines are homozygous *abl* mutant. These females contribute no wild-type Abl to their progeny. When crossed to

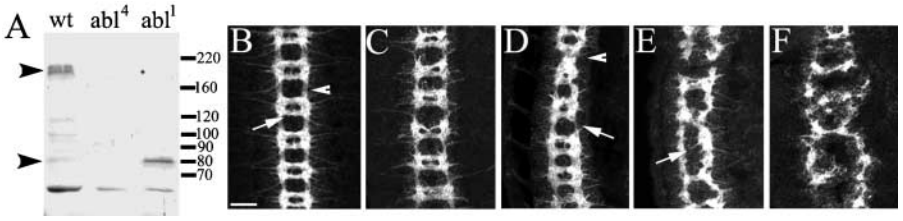

Figure 1. **Complete loss of Abl disrupts CNS development.** (A) Cell extracts from 3-h-old wild-type embryos or embryonic progeny of females with *abl* mutant germlines, immunoblotted with anti-Abl antibody. Wild-type Abl is ~180 kD (top arrow). abl^4 does not produce a protein recognized by this antibody. abl^1 produces a truncated protein product of ~80 kD (bottom arrow). (B–F) Embryos (anterior up) labeled with mAb BP102, which labels all axons. (B) Wild-type CNS, with a scaffold of longitudinal (arrowhead) and commissural (arrow) axons. (C and D) Maternally *abl* mutant but zygotically-rescued embryos have relatively wild-type CNS development, with occasional collapsed longitudinal axons (D, arrowhead) and gaps in axon bundles (D, arrow). (E and F) abl^{MZ} mutants exhibit severe disruptions in CNS development. Most exhibit loss of commissural axons (arrow, E) and some have defects in both longitudinal and commissural axons (F). Bar, 25 μm.

Table I. **Embryonic viability of *abl* maternal and zygotic mutants**

Genotype	Percentage hatched	*n*
abl^1 glc x +/+	92.9	878
abl^4 glc x +/+	89	365
abl^4 glc x shg^2/+	39.5	283[a]
abl^1 glc x shg^2/+	71.1	669[a]
abl^4 glc x shg^{R69}/+	70.4	409[a]
abl^1 glc x scb^2/+	92.3	339[a]
abl^1 glc x abl^1/+	41.0	751[b]
abl^4 glc x abl^4/+	35.6	1149[b]
abl^4 glc; TnAblWT or + x abl^4/+	76	290[c]
abl^4 glc; TnAblK-N or + x abl^4/+	40	299[c]
abl^4 glc; *ena* or +/+ x abl^4/+	61	142[c]
abl^4 glc x shg^2/+; abl^4/+	35.4	398
abl^4 glc x shg^{R69}/+; abl^4/+	38	522

glc, germline clone; TnAblWT, wild-type Abl transgene; TnAblK-N, a kinase-dead Abl trangene (Henkemeyer et al., 1990).
[a]These *shg* or *scb* mutants were balanced with *CyO*.
[b]These *abl* mutants were balanced with TM3.
[c]Only half of the mothers carried the indicated Abl transgene or were heterozygous for *ena*.

abl heterozygous males, half the progeny are maternally and zygotically *abl* mutant, while the other half receive a wild-type copy of *abl* paternally. We used two *abl* alleles: abl^1 produces a truncated protein, and abl^4 is a protein null (Bennett and Hoffmann, 1992; Fig. 1 A). The results were essentially identical with both alleles, and, where tested, were identical when embryos were transheterozygotes.

Embryos lacking both maternal and zygotic Abl (below referred to as abl^{MZ}) die at the end of embryogenesis, while those that receive wild-type paternal Abl survive and go on to adulthood (Table I and unpublished data). Since Abl's role was first defined in the CNS, we examined axon outgrowth using the antibody BP102, which labels all axons of the ventral nerve cord. Zygotic *abl* mutant embryos have subtle defects in CNS development (Wills et al., 1999b). We found that in *abl* maternal mutants that are paternally rescued (identified using a green fluorescent protein [GFP]-marked chromosome), the CNS is normal or has subtle defects (Fig. 1, C and D) which resemble those of *abl dab/abl+* embryos (Gertler et al., 1989). In contrast, maternal/zygotic *abl* mutants have severe defects in CNS development (Fig. 1, E and F). One common feature was a reduction in the commissures which cross the midline. This phenotype resembles that of *abl dab* double mutants (Gertler et al., 1989) and is consistent with previous analysis of the effects of Abl overexpression, which had the opposite effect: enhanced midline crossing (Bashaw et al., 2000). Thus, maternal Abl obscures a role for Abl in CNS axon outgrowth.

We then examined whether Abl plays a role in epithelial development that is obscured by maternally contributed Abl. We first looked at the cuticle, secreted by the epidermal epithelium. abl^{MZ} mutants exhibit defects in three morphogenetic processes, all of which require orchestrated cell shape changes and cell migration: germband retraction, head involution, and dorsal closure (Table II). Approximately 7% of abl^{MZ} mutants completely fail to germband retract or complete head involution (Fig. 2 B), whereas ~14% exhibit partial germband retraction and dorsal closure defects (Fig. 2 C). Approximately 67% of abl^{MZ} mutants have more subtle defects in dorsal closure (Fig. 2, D and F), whereas ~12% are wild-type in appearance or have minor head involution defects. In contrast, *abl* maternal mutants that inherit a paternal wild-type *abl* gene are rescued to normal embryogenesis and adulthood; most hatching larvae are wild-type whereas 5% have slight defects in germband retraction and dorsal patterning. Previous work revealed that certain Abl functions require kinase activity, whereas others do not (Henkemeyer et al., 1990). We found that maternal Abl's role in morphogenesis requires kinase activity, as both the embryonic phenotype and adult viability are rescued by a kinase-active Abl transgene but not by a kinase-dead version (Table I; unpublished data).

One important clue to Abl's function may come from its intracellular localization. Previous work (Bennett and Hoffmann, 1992) documented that *Drosophila* Abl is found in axons of the CNS. Abl is also expressed in epithelial cells, with enrichment in the apical cortical cytoplasm during cellularization, early gastrulation, and in the epithelial cells of the imaginal discs. In later embryos, it is diffuse in the cytoplasm. The original Abl antibody from the Hoffmann lab is no longer available. We attempted to extend this work by generating an anti-Abl polyclonal antibody. This works well on

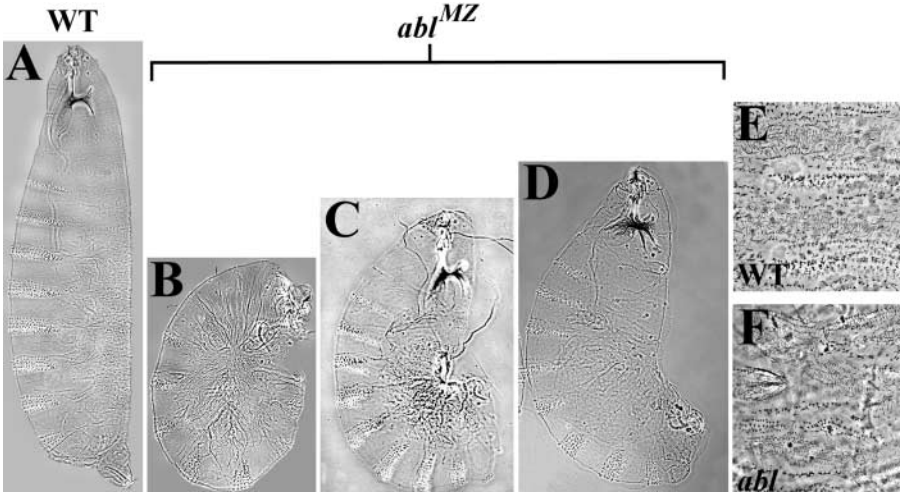

Figure 2. **abl^{MZ} mutants have defects in epithelial morphogenesis.** Cuticle preparations, anterior up. In A–D, dorsal is to the right. (A) Wild-type. (B–D) The range of phenotypes in abl^4 maternal/zygotic mutants, a similar range is observed in abl^1 . (B) Approximately 7% of abl^{MZ} mutants have head involution defects and completely fail to germband retract. (C) ~14% of abl^{MZ} mutants partially fail to germband retract and have variable dorsal closure defects. Note the dorsal hole (arrow). (D) Approximately 67% of abl^{MZ} mutants have dorsal closure defects. (E) Wild-type dorsal hair pattern. (F) Misaligned dorsal hairs in abl^{MZ} mutant.

Table II. **Percentage of dead embryos which have the following defects**

Genotype	U-shaped[a]	Tail-up[b]	Dorsal defects[c]	Wild-type	Dorsal and head defects[d]	*n*
	%	%	%	%	%	
abl^4 glc x +/+			Not applicable as almost all hatch			
abl^4 glc x *shg*^{2}/+	7	2	45	6	40	298
abl^4 glc x *shg*^{R69}/+	10	2	54	2	32	121
abl^4 glc x *abl*^{4}/+	7	14	67	6	6	388
abl^4 glc x *shg*^{2}/+; *abl*^{4}/+	2	5	13	10	70	141
abl^4 glc x *shg*^{R69}/+; *abl*^{4}/+	3	1	60	4	38	307
abl^1 glc x *abl*^{1}/+	1	13	67	17	1	91
abl^1 glc x *scb*^{2}/+; *abl*^{1}/+	3	8	75	10	5	63

[a]Embryos in this class exhibited a complete failure in germband retraction.
[b]Embryos in this class exhibited strong defects in germband retraction and also often had defects in dorsal closure.
[c]Embryos in this class exhibited defects in dorsal closure ranging from dorsal holes to defects in the dorsal pattern.
[d]Embryos in this class exhibited severe defect in head involution; most also showed defects in dorsal closure and/or germband retraction.

immunoblots (Fig. 1 A), but does not show specific staining in situ, as assessed using embryos maternally and zygotically mutant for the protein-null *abl*^{4} (unpublished data).

Loss of Abl disrupts cell migration and cell shape changes during dorsal closure

Previous studies supported a role for Abl in signaling from cell surface receptors to the actin cytoskeleton during axon outgrowth (Wills et al., 1999a; Bashaw et al., 2000). Having identified a role for Abl in epithelial tissues, we hypothesized that Abl might act there by a similar mechanism. One place to address this is during dorsal closure, when lateral epidermal epithelial sheets migrate toward the dorsal midline, enclosing the embryo in epidermis. Dorsal closure involves dynamic actin reorganization to form an acto-myosin purse string in cells at the leading edge of the sheet (Young et al., 1993), as well as orchestrated cell shape changes and cell migration (Kiehart et al., 2000). Since Abl plays a role in dorsal closure, we wondered whether Abl modulates these cellular events.

To compare cell shape changes and cell migration in wild-type and *abl*^{MZ} mutants, we examined embryos during dorsal closure, using antiphosphotyrosine to label both adherens junctions and the leading edge actin cable. As wild-type dorsal closure initiates, leading edge cells elongate uniformly along the dorsal-ventral axis, perpendicular to the leading edge (Fig. 3 A, arrow). As closure proceeds, successive rows of cells lateral to the leading edge also uniformly elongate (Fig. 3, B and C, arrow). The lateral epithelial sheets eventually meet at the dorsal midline, and cells intercalate with one another, making the dorsal surface a continuous epithelial sheet with little midline discontinuity (Figs. 3, D and E, arrow).

abl^{MZ} mutants have striking defects in the cellular events of dorsal closure. Cells fail to change shape in a coordinated fashion (Fig. 3, F–J). As leading edge cells begin to elongate, cells do not elongate uniformly in comparison to their neighbors (Fig. 3, F and G, arrows), and groups of cells have overly broad or narrowed leading edges (arrowheads). As cell shape is likely maintained against tension along the leading edge from the actin cable, altered cell shapes may result from alterations in the polymerization or anchoring of actin (see below). We also observed groups of cells that completely fail to change shape (Fig. 3, G–I, asterisks). As closure proceeds, the cell shape defects persist as cells behind the leading edge begin to elongate (Fig. 3, G–I). Not all *abl*^{MZ} mutants close dorsally, but those that do show a variety of defects at the cellular level. Some embryos maintain groups of cells that have never elongated (Fig. 3 I, asterisks). Other embryos fail to properly align the opposing epithelial sheets at the midline upon completion of closure (Fig. 3 J, arrow), likely contributing to the altered dorsal hair patterning evident in the cuticles (Fig. 2 F). A subset of the *abl*^{MZ} mutants fail to complete germband retraction (Figs. 2 C and 3, K and L). In these embryos, cells along the leading edge exhibit the same cell shape abnormalities during dorsal closure as mutants that complete germband retraction (Fig. 3 L, arrows). A fraction of the cells in *abl*^{MZ} mutants become multinucleate due to defects in cellularization (unpublished data). We verified that cell shape and migration defects during dorsal closure are independent of cell shape disruption due to polyploidy (Fig. 3 O).

The failure to initiate uniform cell shape changes in *abl*^{MZ} mutants is similar to the phenotype we observed in *arm* zygotic mutants (McEwen et al., 2000). These embryos have only maternal Arm, and thus their levels of wild-type Arm are substantially reduced. While *arm* mutants are more severely compromised in their ability to complete dorsal closure than are *abl*^{MZ} mutants, leading edge cells of both *arm* (Fig. 3, M and N) and *abl*^{MZ} mutants fail to elongate uniformly as closure is initiated.

The defects in cell morphology during dorsal closure in *abl*^{MZ} mutants led us to examine localization of actin and of the Abl target Ena, an actin regulator during this process. In the initial stages of dorsal closure, as cells along the leading edge begin to elongate, Ena surrounds the cell membrane but is enriched at vertices of cell–cell contact and at adherens junctions of leading edge cells (Fig. 4 A, left, red). Actin localizes around the entire cell and begins to accumulate at the leading edge at this stage (Fig. 4 A, middle, green; Young et al., 1993). As closure proceeds, Ena accumulates at uniformly high levels in adherens junctions of leading edge cells (Fig. 4 C, left, red), while actin forms a uniform and tightly localized band along the leading edge (Fig. 4 D middle, green).

The localization of both Ena and actin is altered during dorsal closure in *abl*^{MZ} mutants, and these changes parallel the changes in cell shape. As closure initiates, Ena is enriched at adherens junctions, but the level of Ena is not

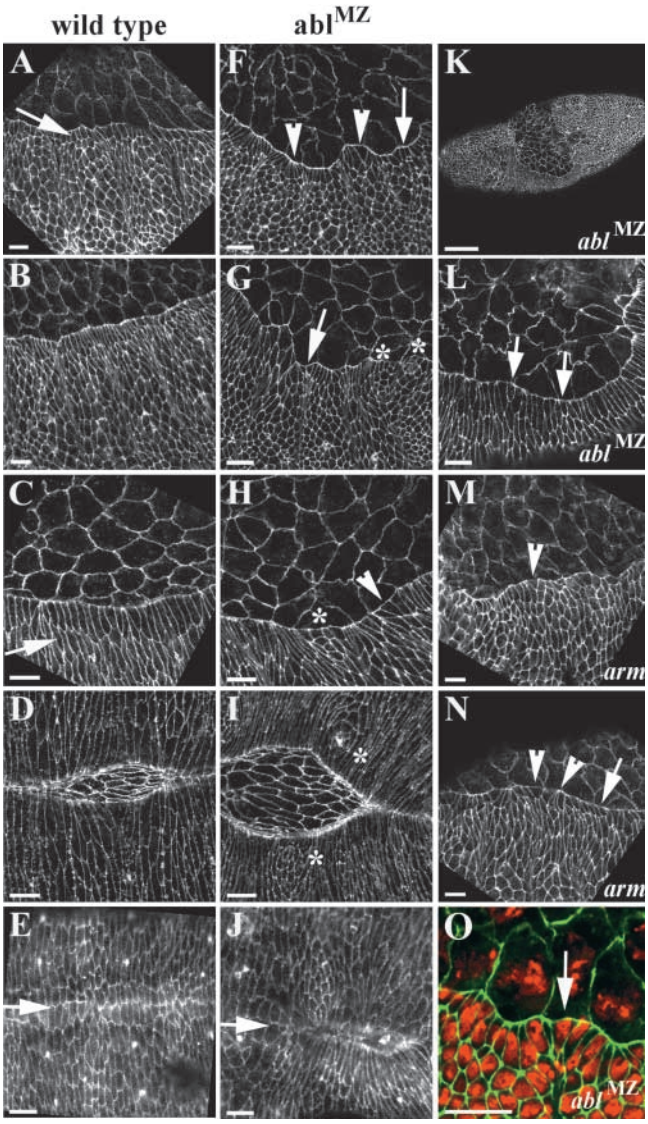

Figure 3. ***abl*^{MZ} mutants fail to undergo coordinated changes in cell shape during dorsal closure.** Embryos labeled with antiphosphotyrosine. Anterior is to the left. (A–E) Wild-type at progressively later stages of dorsal closure. (A–C) Lateral views. (D and E) Dorsal views. (A) Leading edge cells have begun to uniformly elongate (arrow). (B and C) Successive lateral cell rows uniformly elongate (arrow). (D) Lateral epithelial sheets zip together. (E) Closure is complete, with lateral epithelial cells evenly matched at the midline (arrow). (F–J) *abl*^{MZ} mutants at progressively later stages of dorsal closure. (F–H) Lateral and (I–J) dorsal views. (F) Leading edge cells do not elongate uniformly (arrow). Some cells have broadened or constricted leading edges (arrowheads). (G and H) Lateral cells have begun to elongate, but do so nonuniformly (arrow). Some cells have broadened or narrowed leading edges (arrowheads). Other groups of cells completely fail to elongate (asterisks). (I) *abl*^{MZ} mutants that proceeded through dorsal closure. Small groups of cells have still completely failed to change shape (asterisks). (J) *abl*^{MZ} mutant that completed closure. Epithelial sheets often fail to align properly at the midline (arrow). (K and L) Some *abl*^{MZ} mutants initiate dorsal closure even though they have not completed germband retraction. Cell shape defects are also seen in these embryos (arrows). (M and N) *arm*^{XP33} mutants have cell shape defects similar to *abl*^{MZ} mutants. Cells fail to elongate uniformly (arrow) and have broadened or narrowed leading edges (arrowheads). (O) Cell shape defects in *abl*^{MZ} mutants are not caused by multinucleate cells. *abl*^{MZ}, double-labeled with antiphosphotyrosine and with propidium iodide, labeling nuclei. Mononucleate cells have defects in shape (arrow). Bars: (A–J and L–O) 10 μm; (K) 50 μm.

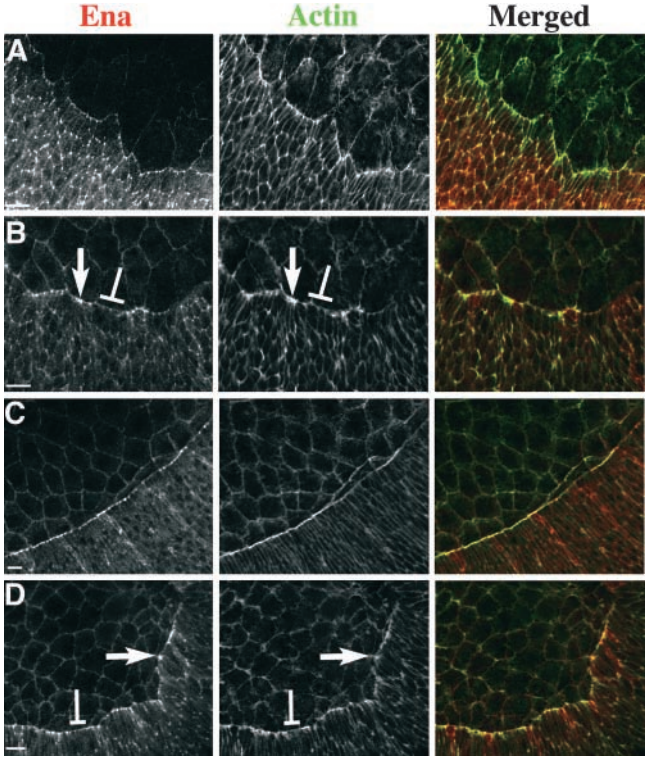

Figure 4. **Complete loss of Abl alters Ena and actin localization during dorsal closure.** Lateral view. Embryos double-labeled with anti-Ena (red) and phalloidin (green), labeling F-actin. (A) Stage 13 wild-type embryo with leading edge cells initiating elongation. Ena (left, red) is enriched at vertices of cell–cell contact. Actin (middle, green) outlines all cell membranes and is beginning to accumulate at the leading edge. Actin and Ena colocalize at cell junctions. (B) Stage 13 *abl*^{MZ} mutant. Ena (left, red) and Actin (middle, green) enrichment is not uniform at the leading edge. Both are enriched in some cells (arrows) and depleted in others (brackets). (C) Stage 14 wild-type embryo. More lateral cells have undergone uniform elongation. Ena is uniformly enriched at adherens junctions of leading edge cells (left, red). Actin forms a tight cable along the leading edge (middle, green). Ena and actin colocalize at adherens junctions as actin expands along the entire leading edge. (D) Stage 14 *abl*^{MZ} mutant. Nonuniform localization of Ena and Actin persists. Cells with excess Ena (left, arrow) often accumulate excess Actin (middle, arrow), whereas cells with diminished Ena levels (left, bracket) have diminished levels of Actin (middle, bracket) Bars, 10 μm.

uniform in different cells (Fig. 4 B, arrow vs. bracket). The actin cable is also not uniform; levels of actin often change in parallel to Ena (Fig. 4 B). This uneven distribution of Ena and actin persists throughout dorsal closure (Fig. 4 D). Changes in Ena and actin levels often correlate with defects in cell shape. Cells with constricted leading edges tend to accumulate abnormally high levels of both proteins, whereas cells with broadened leading edges tend to have lower levels of Ena in junctions and lower levels of leading edge actin. This correlation may be explained by the fact that the leading edge is under tension, presumably due to the contractile actin cable (Kiehart et al., 2000). Defects in actin cable assembly or anchoring within individual cells could lead those cells to splay open at the leading edge; adjacent cells might then hypercontract due to the release of the tension normally exerted by their neighbors.

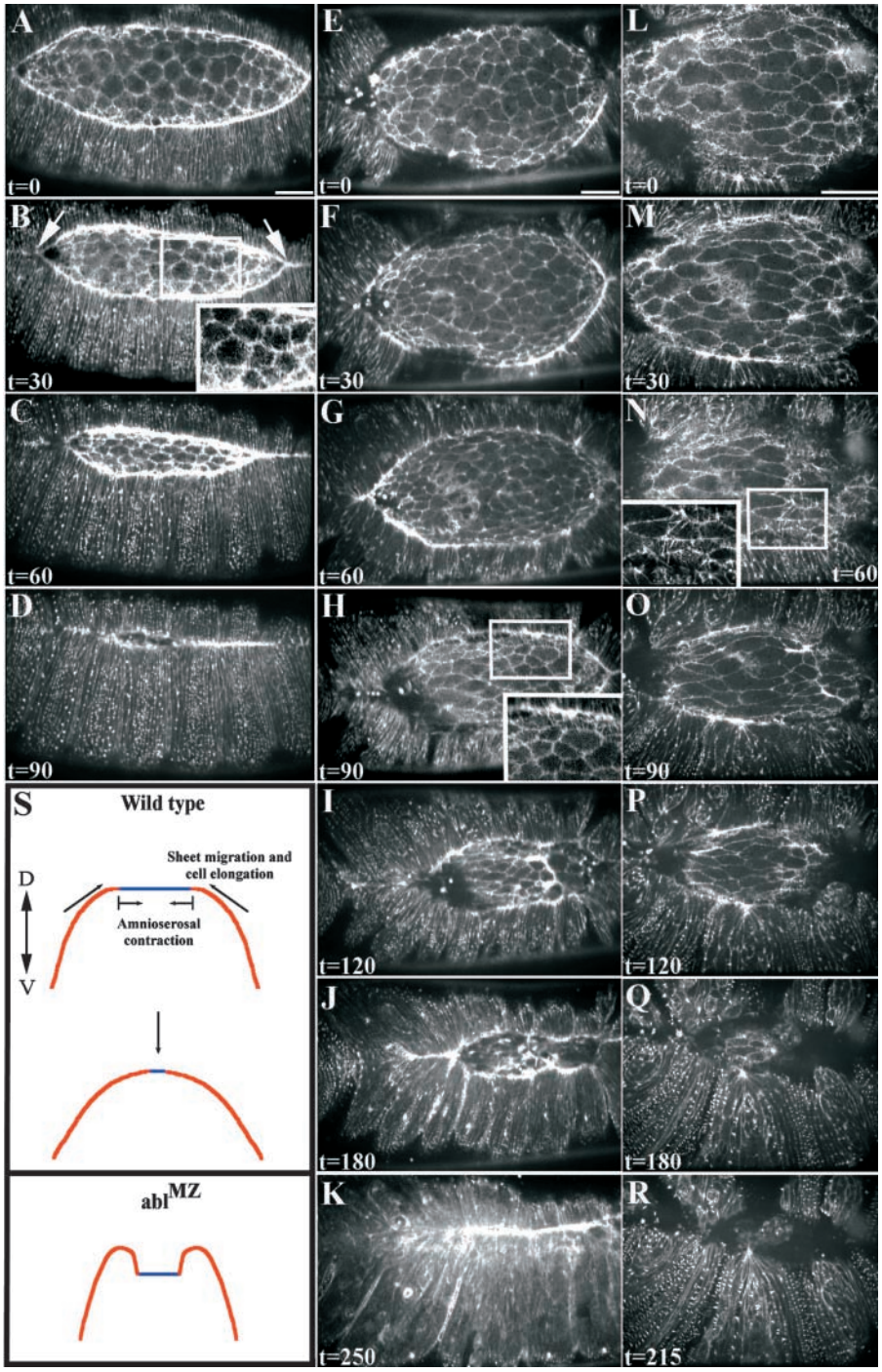

Figure 5. **Dorsal closure is substantially slowed in *abl*^{MZ} mutants.** Dorsal view of embryos expressing moesin-GFP, anterior to the right. Time is in minutes. Insets in (B, H, and N) display actin-rich filopodia extending from amnioserosa or leading edge cells. (A–D) Wild-type embryo at 30 min intervals during dorsal closure. (A) The leading edge of the dorsal closure front is uniformly enriched in actin. Lateral epithelial sheets elongate uniformly. (B) 30 min. Amnioserosa cells are undergoing apical constriction and the embryo is zipping together at the anterior and posterior ends (arrows). (C) 60 min. Amnioserosa cells have constricted apically and remain in the same plane of focus as the lateral epithelial sheets. (D) 90 min. Dorsal closure is complete. (E–K) *abl*^{MZ} mutant. The amnioserosa cells in E are comparable in surface area to the wild-type in A. (F–H) As closure progresses, amnioserosa cells constrict and lateral epithelial cells elongate, but dorsal closure is delayed relative to wild-type (compare D and H). If one matches embryos based on the length of the leading edge (compare A and G), closure is still delayed. This embryo took >4 h to complete closure (K). (L–R) A different *abl*^{MZ} mutant at higher magnification, illustrating the folding-under of the leading edge and failure to complete closure. (S) Cross-section diagram depicting one interpretation of the defects of *abl*^{MZ} mutants. In wild-type embryos, the rate at which lateral cells elongate, the sheets migrate, and amnioserosa cells constrict are tightly coordinated. In *abl*^{MZ} mutants, the leading edge folds under the more lateral epidermis, perhaps because leading edge cells migrate too slowly or amnioserosa cell constriction is slowed (these events are likely coupled), forcing the sheet to fold under. Time-lapse videos supplementing this figure are available at http://www.jcb.org/cgi/content/full/jcb.200105102/DC1. Bars, 25 μm.

Dorsal closure is slowed in *abl* mutants

Multiple forces drive dorsal closure, including forces generated by cell shape changes, contraction of the leading edge actin-myosin cable, and pulling forces exerted by amnioserosa cells. These forces act combinatorially, so disruption of one force slows but does not prevent closure (Kiehart et al., 2000). *abl*^{MZ} mutants display defects in both cell shape and in the actin cable, yet many embryos complete closure, albeit imperfectly. To analyze how *abl*^{MZ} mutants compensate for disruptions in cell shape and the actin cable, we performed time-lapse confocal microscopy on embryos undergoing closure (see videos available at http://www.jcb.org/cgi/content/full/jcb.200105102/DC1). We analyzed transgenic flies expressing the actin binding domain of Moesin fused to GFP (Kiehart et al., 2000), allowing us to visualize actin dynamics in real time.

During dorsal closure in living wild-type embryos, the leading edge becomes uniformly enriched in actin as leading edge cells elongate (Fig. 5 A). Amnioserosa cells, the large squamous cells exposed on the dorsal surface of the embryo, undergo apical constriction (Kiehart et al., 2000), decreasing in surface area throughout closure (Fig. 5, A–D). Finally, as the lateral epithelial sheets migrate toward one another, closure is initiated at the anterior and posterior ends of the opening (Fig. 5 B, arrows) and the sheets zip together from the ends (Fig. 5, A–D) (Jacinto et al., 2000). Once the cells

initiate elongation and the front is enriched in actin, dorsal closure is completed in a little over 1.5 h.

Dorsal closure is substantially slowed in abl^{MZ} mutants. It is not simple to define an equivalent starting point for abl^{MZ} and wild-type embryos, as the dorsal/ventral extent of the amnioserosa is larger in abl^{MZ} mutants, both in cell number and distance (compare Fig. 5 A to E). This may be due to defects in cell rearrangements during germband retraction. However, regardless of whether we compared embryos with equivalent amnioserosa surface areas (Fig. 5 A vs. E) or with roughly equivalent length leading edges (Fig. 5 A vs. G), closure is substantially delayed in abl^{MZ} mutants, taking two to three times longer than normal. At the cellular level, lateral cells elongate on schedule in the mutants (despite defects in cell shape) and amnioserosa cells apically constrict, though more slowly than in wild-type.

Time-lapse imaging also revealed defects that were not apparent in our fixed images. As closure proceeds, the leading edge of the lateral epidermis folds under the more lateral cells that follow it (Fig. 5, J, Q, and R). This suggests that while lateral epithelial cells continue to elongate and migrate, driving sheet extension, leading edge cells do not migrate toward one another at an appropriate rate (diagram in Fig. 5 S). Our movies also suggest that filopodial extensions from the leading edge might aid in the eventual closure, as they do in wild-type (Jacinto et al., 2000), actively zipping the epidermal sheets together. Filopodial extensions from epidermal and amnioserosa cells are present in both wild-type and abl^{MZ} mutants, and even appear more fre-

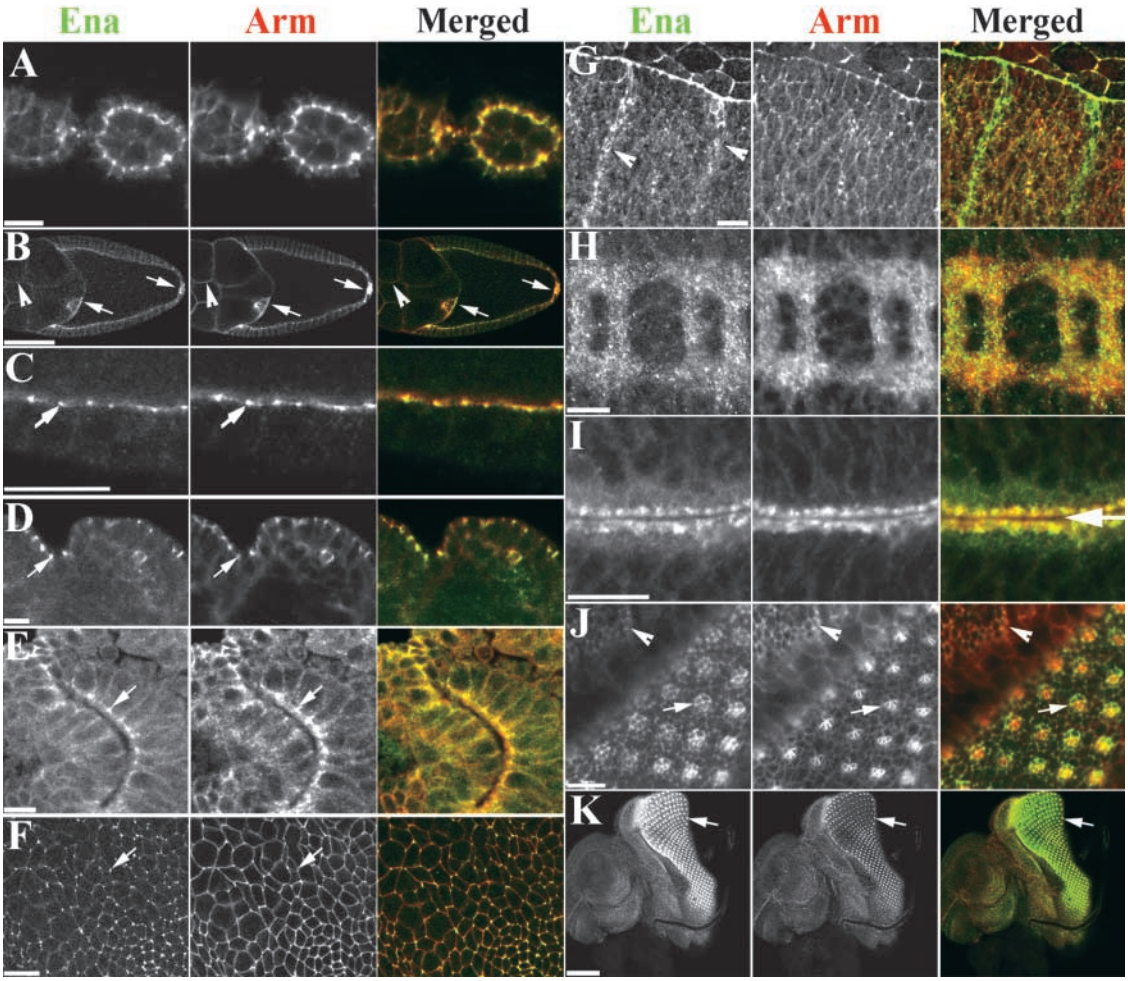

Figure 6. **Ena and Arm colocalize at adherens junctions throughout development.** All images (except I) are anterior to the right. Ena is green and Arm is red in merged images. (A) Stage 3 egg chamber. Ena and Arm are enriched in apical adherens junctions of follicle cells. (B and C) Stage 10 egg chamber. Levels of Ena and Arm drop, but both remain at adherens junctions. Anterior (border cells) and posterior polar follicle cells are enriched in both Ena and Arm (B, arrows). Ena and Arm also colocalize to nurse cell membranes (B, arrowhead). (D–G) During embryogenesis Ena and Arm colocalize to adherens junctions of epithelial tissues. (D) Cross-section, stage 9 embryo. Ectodermal adherens junctions (arrow). (E) Adherens junctions of polarized cells of the invaginating hindgut (arrow). (F) Apical view, stage 9 embryo. Ena is enriched at vertices of cell–cell contact (arrow), whereas Arm is more uniform. (G) During dorsal closure Ena is enriched at adherens junctions of leading edge cells, but it is also found in the cytoplasm of cells at the segment boundary (arrowheads). (H) Ena and Arm both localize to axons. (I–K) Imaginal discs. (I) Apical surfaces of two epithelial sheets opposed to one another in the wing imaginal disc (arrow). Ena and Arm colocalize to apical adherens junctions, and are also found at the apical surface. (J and K) In eye imaginal discs cell differentiation occurs after the morphogenetic furrow passes. In undifferentiated cells, Ena and Arm colocalize to cell boundaries (J, arrowhead). As groups of cells begin differentiating as photoreceptors (J, arrow), Ena localizes uniformly to all cells of the precluster. Arm, in contrast, accumulates at high levels in a subset of these cells. Later, Ena and Arm colocalize in photoreceptor rhabdomeres (K, arrow). Bars: (A–J) 10 μm; (K) 50 μm.

quent in late-stage mutants (Fig. 5, B, H, and N, insets). We suspect epithelial sheet migration is compromised in *abl* mutants due to the discontinuity of the leading edge actin cable and the cell shape defects. In this situation, filopodia may be needed to locate the opposing epidermis and eventually zip up the embryo.

ena suppresses the *abl* phenotype and localizes to adherens junctions

The best characterized substrate of *Drosophila* Abl is Ena. Mutations in *ena* suppress the effects of *abl dab* mutations (Gertler et al., 1995). We thus examined whether *ena* might act with Abl in epithelial morphogenesis. Data from the Hoffmann lab supported this possibility: they found that females homozygous for *abl* mutations, which are normally sterile, become fertile when they are also heterozygous for *ena* (Bennett and Hoffmann, 1992). We thus generated homozygous *abl* germline clones in females that were heterozygous for *ena* (for experimental reasons only 50% of the females generated in the experiment are *ena* heterozygotes) and crossed them to *abl* heterozygous males. *ena* heterozygosity significantly rescued the abl^{MZ} embryonic lethality (Table I).

These data suggest that Ena misregulation contributes to the defects in morphogenesis we observed in abl^{MZ} mutants. We thus examined Ena localization in epithelial tissues, as this might reveal, at least in part, where Abl is acting. We used two different anti-Ena antibodies (Gertler et al., 1995; Bashaw et al., 2000) with similar results. We found that Ena colocalizes with Arm at adherens junctions throughout most stages of development. During early oogenesis, Ena and Arm are strongly enriched at adherens junctions of follicle cells surrounding the germline (Fig. 6 A; Baum and Perrimon, 2001) and remain enriched at junctions, though at lower levels as oogenesis proceeds (Figs. 6, B and C). During embryogenesis, Ena begins to accumulate in adherens junctions at the onset of gastrulation (unpublished data) and colocalizes with Arm at adherens junctions in germband-extended embryos (Fig. 6 D, arrow) and in fully polarized cells, such as the invaginating hindgut (Fig. 6 E, arrow). Arm localizes uniformly around cells (Fig. 6 F), whereas Ena, though present all around the plasma membrane, is enriched at vertices of cell–cell contact (Fig. 6 F, arrow). Ena is strongly enriched in adherens junctions of leading edge cells during dorsal closure (Figs. 4 C and 6 G), and also localizes to the cytoplasm in a stripe of epidermal cells at the segmental boundary (Fig. 6 G, arrowheads). Ena and Arm also localize to CNS axons (Gertler et al., 1990; Fig. 6 H). During larval development, Ena and Arm are strongly enriched at adherens junctions of the highly polarized imaginal disc epithelia, precursors of the adult epidermis (Figs. 6 I, arrow), as well as in the specialized junctions of the photoreceptor rhabdomeres (Fig. 6, J and K). Thus, Arm and Ena colocalize in adherens junctions in most epithelial cells.

ena and *arm* genetically interact during dorsal closure

Our genetic experiments suggest that Ena misregulation plays a role in the defects in morphogenesis of abl^{MZ} mutants (Table I). As Ena localizes to adherens junctions, we wondered whether it might work with adherens junction components during morphogenesis. We thus looked for genetic interactions between *ena* and *arm*. We crossed females heterozygous for mutations in both *arm* and *ena* to males heterozygous for *ena.* Both *arm* and *ena* are embryonic lethal; as *arm* is on the X-chromosome, we expect 43% of the dead progeny to be *arm* mutant, 43% to be *ena* mutant, and 14% to be *arm; ena* double mutants. Null alleles of Arm have dorsal closure defects, due to a combination of affects on cell adhesion and Wg signaling (McEwen et al., 2000), whereas weaker *arm* alleles do not have dorsal closure defects. We first tested the weakest allele of *arm,* $arm^{H8.6}$, in which dorsal closure is normal, although segment polarity is affected (Fig. 7 B). Although *ena* homozygotes are embryonic lethal, most of the dead embryos only have mild defects in head involution (Gertler et al., 1990; Fig. 7 C). A small fraction (~5%) have dorsal pattern defects indicative of mild problems in dorsal closure. When we generated $arm^{H8.6}$; ena^{GC1} double mutants, we found strong synergistic defects in both head involution and dorsal closure (Fig. 7 D; Table III). Mutations in *ena* also enhance the dorsal closure defects of the stronger *arm* mutants arm^{XM19}, arm^{XP33} (unpublished data), and arm^{YD35} (Fig. 7, E and F; Table III), though it is difficult to rule out the possibility that these interactions are simply additive.

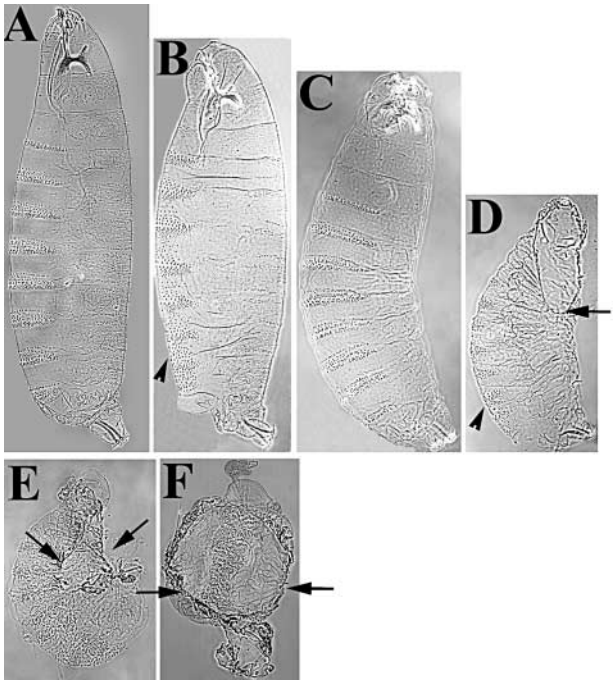

Figure 7. **Mutations in *ena* enhance *arm*'s dorsal closure defects.** Cuticle preparations, anterior up. (A) Wild-type. (B) $arm^{H8.6}$ mutants have segment polarity defects due to defects in Wingless signaling (arrowhead), but head involution and dorsal closure are normal. (C) ena^{210}/ena^{GC1}. (D) $arm^{H8.6}/Y$; ena^{GC1}/ena^{GC1}. Note strong defects in dorsal closure and head involution (arrow), with no change in the segment polarity phenotype (arrowhead). (E) arm^{YD35} mutants have a dorsal hole (arrows), as well strong segment polarity defects. (F) The dorsal side of arm^{YD35}; ena^{210}/ena^{210} embryos is completely open (arrows).

Table III. ***arm* and *ena* genetically interact**

Cross	Percentage of dead embryos with:			n
	***arm* ø-type**	***ena* ø-type**	***arm; ena***	
$arm^{H8.6}$/+; ena^{GC1}/+ × +/Y; ena^{GC1}/+	34	53	13	218
arm^{YD35}/+; ena^{GC1}/+ × +/Y; ena^{GC1}/+	51	35	14	635
Predicted by Mendelian ratios	43	43	14	

Mutations in DE-cadherin enhance the *abl* phenotype

The genetic interactions between *arm* and *abl* in the CNS and epidermis (Loureiro and Peifer, 1998) and the localization of Ena to adherens junctions suggest that Abl might act in part at adherens junctions. In cultured mammalian cells Abl localizes to cell–matrix junctions (Lewis et al., 1996). As one test of the possible sites of Abl action during morphogenesis, we looked for dose-sensitive genetic interactions between *abl* and genes encoding proteins involved in epithelial adhesion: DE-cadherin (encoded by *shotgun* (*shg*); Tepass et al., 1996; Uemura et al., 1996), which mediates cell–cell adhesion, and *scab* (*scb*), an integrin α-chain which mediates cell-matrix adhesion during dorsal closure (Stark et al., 1997).

We saw strong genetic interactions of *abl* with the cadherin *shg*, but not with the integrin *scb*. We crossed females with *abl* mutant germlines to males heterozygous for *shg* or *scb*. All progeny lack maternal Abl and are zygotically *abl* heterozygous, receiving a wild-type copy paternally. Zygotic wild-type Abl normally rescues all of these embryos to viability (Table I). However, shg^2 heterozygosity led to lethality of *abl*/+ embryos (Table I). Only 40% of the progeny hatch, and the dead embryos have dorsal closure and germband retraction defects similar to abl^{MZ} mutants. Many also have severe defects in head involution (Fig. 8 B, arrow). Similar, though somewhat less penetrant, results were seen with the *shg* null allele, shg^{R69} (Table I). In contrast, we saw no effects on the survival of *abl*/+ embryos of removing one copy of *scb* (Table I). To increase the sensitivity of this genetic interaction assay, we crossed females with *abl* mutant germ lines to *abl*/+; *shg*/+ or *abl*/+; *scb*/+ males. Half of the progeny lack both maternal and zygotic Abl, and half of those are also heterozygous for either *shg* or *scb*. Heterozygosity for shg^2 substantially enhanced the abl^{MZ} phenotype (Fig. 8 D; Table II). Approximately half of the dead embryos (presumably those that were *abl/abl;* shg^2/+) had a prominent dorsal anterior hole not seen in abl^{MZ} mutants (Fig. 8 D); these embryos also had the typical spectrum of dorsal closure and germband retraction defects. We saw similar phenotypic enhancement in abl^{MZ} embryos heterozygous for the *shg* null allele, shg^{R69}. (Fig. 8 E; Table II). In contrast, this sensitized assay did not uncover a significant genetic interaction between *abl* and *scb* (Table II).

Loss of Abl decreases the amount of junctional arm and α-catenin

The genetic interactions between *abl* and *shg* suggested that some of the morphogenesis defects observed could result from effects of Abl at adherens junctions. Alternately, they might result from more nonspecific effects on cell polarity or the cytoskeleton. We thus examined the subcellular localization of adherens junction proteins and other markers of cell polarity in abl^{MZ} mutants. To control for variability between experiments, we analyzed mixed populations of wild-type and mutant embryos that had undergone simultaneous fixation, staining, and microscopy. We used a wild-type strain carrying a GFP transgene, allowing us to unambiguously discriminate between wild-type and mutant embryos. The mutant embryos had fathers which were heterozygous for *abl* and a different GFP-transgene, to differentiate abl^{MZ} from paternally rescued embryos.

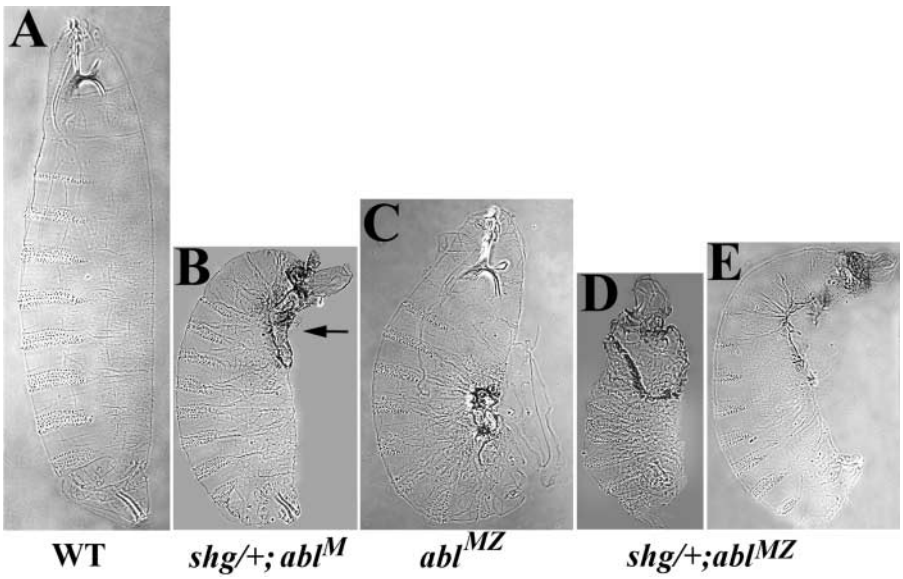

Figure 8. **DE-cadherin (*shg*) genetically interacts with Abl.** Cuticle preparations, anterior up. (A) Wild-type. (B) abl^4/abl^4 × shg^2/*CyO*. abl^4 maternal mutants are zygotically rescued, with all hatching as larvae and most appearing wild-type. *shg* heterozygosity prevents zygotic rescue of *abl* maternal mutants and leads to morphogenesis defects. Note defects in dorsal closure and head involution (arrow). (C) abl^{MZ} mutants die during embryogenesis with defects in epithelial morphogenesis. (D and E) *shg* heterozygosity enhances the abl^{MZ} phenotype. (D) 70% of lethal progeny of abl^4/abl^4 × shg^2/+; abl^4/+ have cuticles that are reduced in size with a large dorsal-anterior hole. (E) 30% of the lethal progeny of abl^4/abl^4 × shg^{R69}/+; abl^4/+ have a prominent dorsal-anterior hole.

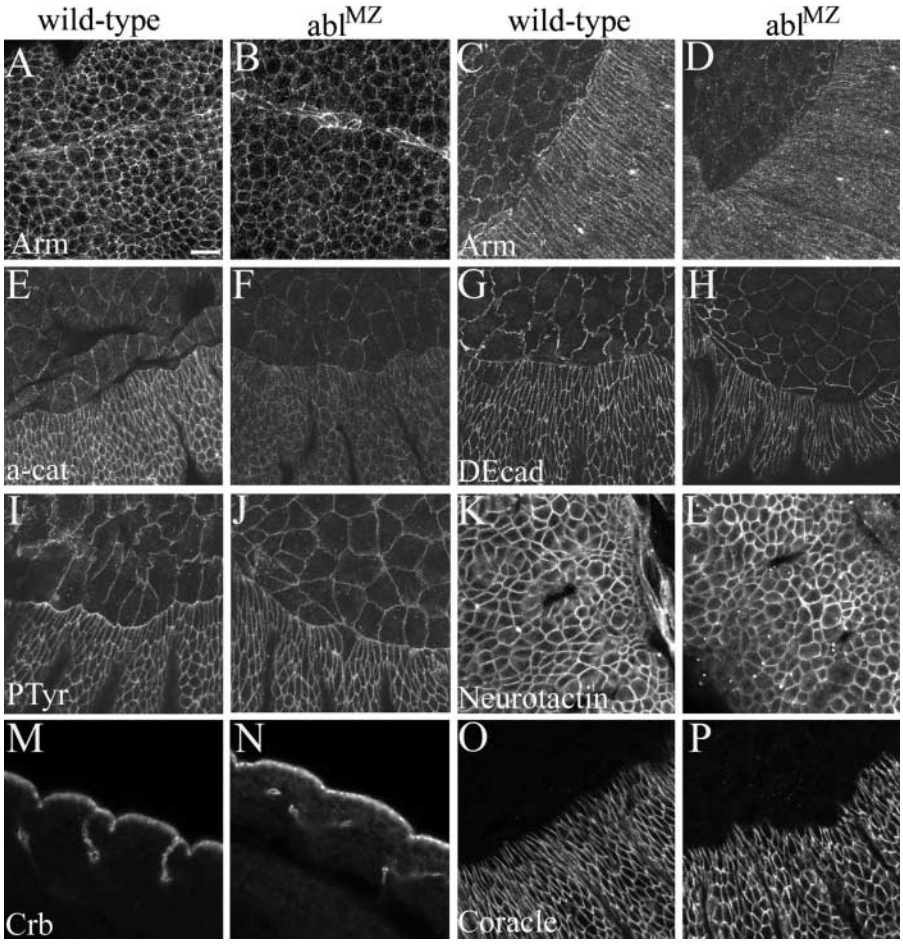

Figure 9. **Levels of junctional Arm and α-catenin are reduced in *abl*^{MZ} mutants.** Embryos labeled with anti-Arm (A–D), anti–α-catenin (E and F), anti–DE-cadherin (G and H), antiphosphotyrosine (I and J), anti-Neurotactin (K and L), anti-Crumbs (M and N), and anti-Coracle (O-P). (A and B) Stage 8. (C and D) Stage 14. (A and C) Wild-type. Arm localizes to adherens junctions. (B and D) *abl*^{MZ} mutants. Arm accumulates at reduced levels in adherens junctions. (E and F) Stage 13. (E) Wild-type. α-catenin localizes to adherens junctions. (F) *abl*^{MZ} mutant. α-catenin accumulates at reduced levels in adherens junctions. (G–J) Stage 13. DE-cadherin localizes to adherens junctions, without striking differences in localization or levels between wild-type (G) and *abl*^{MZ} mutants (H). Phosphotyrosine localizes to adherens junctions, without noticeable differences between wild-type (I) and *abl*^{MZ} mutants (J). (K and L) Stage 11. Neurotactin localizes to the baso-lateral membrane without noticeable differences between wild-type (K) and *abl*^{MZ} mutants (L). (M and N) Cross-sectional views, Stage 11. Crumbs localizes to the apical membrane of epithelial cells without striking differences between wild-type (M) and *abl*^{MZ} mutants (N). (O and P) Stage 13. Coracle localizes to septate junctions with no striking difference in levels between wild-type (O) and *abl*^{MZ} mutants (P). Bar, 10 μm.

abl^{MZ} mutants had reduced levels of Arm in adherens junctions. This was first noticeable in germband-extended embryos (Fig. 9, A and B) and became more pronounced during dorsal closure in wild-type (Fig. 9, C and D). Cross-sectional views suggest that the decrease in Arm at adherens junctions is not due to mislocalization of Arm to a different place in the cell (unpublished data), and we also think it is unlikely to be solely due to the alterations in cell shape in the mutant. Given these effects on Arm, we analyzed other adherens junction components. α-catenin, a protein that links Arm to the actin cytoskeleton, also showed reduced accumulation in adherens junctions (Fig. 9, E and F). The localization of both Arm and α-catenin was more variable in paternally rescued embryos, with reduction in some individuals but not others (unpublished data). The accumulation of DE-cadherin at junctions also may be slightly reduced in *abl*^{MZ} mutants (Figs. 9, G and H), but this effect was less pronounced than that on Arm or α-catenin. We also examined several other cortical or membrane markers. The accumulation of phosphotyrosine in adherens junctions (Fig. 9, I and J), Coracle at septate junctions (Fig. 9, O and P), Neurotactin at the basolateral membrane (Fig. 9, K and L), and Crumbs at the apical membrane (Fig. 9, M and N) were only slightly reduced or unaffected. In doing these experiments, we also observed that the defects in cell shape in *abl*^{MZ} mutants are not restricted to dorsal closure. We observed defects in the uniform apical constrictions that occur in cells along the ventral midline (Fig. 9, A and B). Defects in cell shape changes and cell migration could also explain the observed defects in germband retraction.

To complement these immunofluorescence assays, we examined total protein levels of Arm and other proteins in the progeny of *abl*^{4} germline mutant females crossed to *abl* heterozygous males. Half of these embryos are *abl*^{MZ} and the other half are zygotically rescued. To ensure that embryos were similarly aged and to remove unfertilized eggs from the samples, we selected living embryos at the cellular blastoderm stage and then let them develop for given amounts of time. Total levels of Arm protein are significantly reduced throughout development compared with wild-type (Fig. 10, A–C). Similar reductions in Arm protein were observed in *abl*^{1} (unpublished data). In contrast to Arm, the levels of two unrelated control proteins, Pnut and BicD, were unaffected by loss of Abl function (Fig. 10, A–C). We next examined the levels of other adherens junction proteins. Reduction in Abl function also led to reduction in α-catenin protein levels (Fig. 10 A). In contrast, levels of DE-cadherin are not altered in *abl* mutants (Fig. 10, A–C). We then assessed whether these effects were specific for adherens junction proteins, by examining the levels of other markers of cell polarity or the cytoskeleton. We saw either subtle reduction or no effect of *abl* mutations on the levels of actin, the septate junction protein Coracle, and the apical marker Crumbs (Fig. 10, B and C).

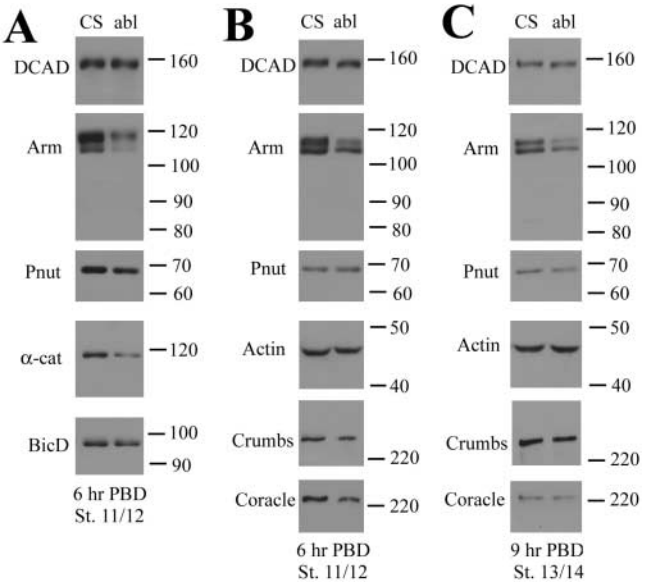

Figure 10. **Total levels of Arm and α-catenin are reduced in *abl* mutants.** *abl* germline mutant females were mated to *abl* heterozygous males and progeny were picked at the cellular blastoderm stage and aged for the indicated time postblastoderm (PBD). Wild-type embryos (Canton S [CS]) served as a control. Cell extracts were fractionated by SDS-PAGE and immunoblotted with the indicated antibodies. Molecular weight markers are to the right. Bicaudal D (BicD) or Peanut (Pnut) are loading controls. Each vertical set of samples represents sequential reprobing of the same blot. (A and B) Stage 11/12 embryos (6 h postblastoderm). (C) Stage 13/14 embryos (9 h postblastoderm).

Discussion

Activation of Abl tyrosine kinase plays a key role in the development of certain human leukemias (for review see Zou and Calame, 1999). Despite the attention paid to its role in oncogenesis, the complex roles Abl plays in normal cells are not as well understood. Here we report a novel role for Abl in epithelial cells, in which it regulates cell shape changes and cell migration during epithelial morphogenesis in vivo. These data may have broader implications, providing insights into the possible underlying cause of some of the defects seen in the mouse *abl* mutants and *abl; arg* double mutants, and may also provide insight into the role Bcr-Abl plays in leukemic cells. Further, these data provide in vivo evidence for a role for a tyrosine kinase in epithelial morphogenesis. This has been suspected from the actions of activated kinases in cultured cells (for review see Daniel and Reynolds, 1997), but our experiments test this in the intact animal.

It is useful to compare what we observed in the epidermis with Abl's role in axon outgrowth, where it is thought to modulate communication between at least two transmembrane axon guidance receptors, Robo and dLAR, and the actin cytoskeleton (for review see Lanier and Gertler, 2000). Abl is thought to antagonize Ena in this process. The *ena* and *abl* phenotypes were surprising in one respect. Ena/VASP proteins had been thought to enhance actin polymerization based on promotion of intracellular motility of the bacteria *Listeria*. However, while promoting actin polymerization might be expected to drive growth cone extension and axon outgrowth, Ena promotes growth cone repulsion and axon stalling (Bashaw et al., 2000; Wills et al., 1999a,b), whereas Abl has opposite effects. Work in cultured fibroblasts led to similar conclusions: Ena/VASP proteins inhibit cell migration (Bear et al., 2000).

Building on this model, Abl and Ena might play analogous roles in epithelial cells, translating extracellular signals into changes in the actin cytoskeleton. This sort of cytoskeletal modulation plays a key role in cell migration and cell shape changes during epithelial morphogenesis. One model consistent with our data is that Abl acts at adherens junctions during morphogenesis. Cadherins and catenins play important roles in morphogenesis in all animals. Severe reduction in *Drosophila* Arm (Cox et al., 1996) or DE-cadherin (Tepass et al., 1996) function leads to early loss of epithelial integrity. Less severe reduction in cadherin/catenin function affects head involution, dorsal closure, and other morphogenetic processes (Tepass et al., 1996; Uemura et al., 1996; McEwen et al., 2000). In fact, many epithelial defects of *DE-cadherin* mutants are blocked by blocking morphogenetic movements (Tepass et al., 1996), suggesting that modulating adhesion is critical to morphogenesis.

Several lines of evidence support the possibility that the morphogenetic defects of abl^{MZ} mutants result, at least in part, from Abl action at adherens junctions. First, the effects on dorsal closure, germband retraction, and head involution are strongly enhanced by reducing the dose of DE-cadherin. Second, the defects in cell shape during dorsal closure resemble, in part, those of *arm* mutants. Third, the defects in morphogenesis are suppressed by mutations in *ena*, which is primarily found at adherens junctions. Finally, we observed a reduction in junctional Arm and α-catenin in abl^{MZ} mutants. It is important to note, however, that any role for Abl at adherens junctions would be a modulatory one. It is not absolutely essential for adherens junction assembly or function. Of course, it remains possible that other tyrosine kinases may act redundantly with Abl. The relationship between the cadherin-catenin system, Abl, and Ena that may occur in epithelial cells could also exist in the CNS. Arm and DN-cadherin play roles in axon outgrowth in *Drosophila*, and in this role *arm* interacts genetically with *abl* (Iwai et al., 1997; Loureiro and Peifer, 1998).

One target of Abl might be Ena, which could regulate actin dynamics in the actin belt underlying the adherens junction. Just as local modulation of actin dynamics likely regulates growth cone extension or stalling, the cell shape changes and cell migration characteristic of morphogenesis will require modulation of actin dynamics and junctional linkage. The idea that Ena may regulate cell–cell adhesion recently received strong support from work in cultured mammalian keratinocytes, where inhibiting Ena/VASP function prevented actin rearrangement upon cell–cell adhesion (Vasioukhin et al., 2000). This model was further supported by work published while our paper was under review, which demonstrated that both Ab1 and Ena regulate actin polymerization at the adherens junctions of ovarian follicle cells in *Drosophila* (Baum and Perrimon, 2001).

Other models are also consistent with our data. Abl may act directly on the actin cytoskeleton, with its effects on

junctions a more indirect consequence. Junctional linkage to actin is critical for effective cell adhesion (Hirano et al., 1992) and alterations in actin polymerization could affect the ability to assemble stable cadherin–catenin complexes, as was observed in cultured mammalian cells (Quinlan and Hyatt, 1999), resulting in the observed loss of Arm from junctions. Abl could also play a more general role in the establishment and maintenance of cell polarity. Finally, studies of cultured mammalian cells also suggest that Abl acts at cell-matrix junctions to modulate responses to integrin-mediated adhesion by associating with and phosphorylating focal adhesion proteins like paxillin and Crkl (for review see Van Etten, 1999). In doing so, it may influence both tethering to actin and signal transduction. *Drosophila* integrins play important roles in morphogenetic processes such as dorsal closure and germband retraction (for review see Brown et al., 2000). We did not detect genetic interactions between *abl* and *scab*, the integrin α-chain that plays a role in dorsal closure (Stark et al., 1997). However, this does not rule out interplay between integrins and Abl in morphogenesis. It is now important to test these different models by investigating the mechanism by which Abl and Ena act during morphogenesis.

Materials and methods

Fly stocks and phenotypic analysis

All mutations are described in Flybase (http://flybase.bio.indiana.edu/). abl^1 and abl^4 germ line clones were generated by the FLP dominant female sterile technique (Chou and Perrimon, 1996). 48–72-h-old *hsflp:abl FRT 79D-F/ovo*^{D1} *FRT 79D-F* larvae were heat shocked for 3 h at 37°C. Only homozygous *abl* mutant germ cells develop in these females. Stocks to generate *abl* germ line clones, *hsflp;Dr*^{MIO}*/TM3*, *FRT3L79D-F/TM3*, and *ovo*^{D1} *FRT3L79D-F/TM3*, were from the Bloomington *Drosophila* Stock Center. *abl* and *ena* alleles were from M. Hoffmann (University of Wisconsin, Madison, WI). The wild-type was Canton-S. Transgenic lines expressing *histone-GFP,* the actin binding domain of Moesin fused to GFP (Kiehart et al., 2000), or *UAS-GFP* under the control of *sim-GAL4* were provided by R. Saint (University of Adelaide, South Austrailia, Austrailia), D. Kiehart (Duke University, Durham, NC), and S. Crews (University of North Carolina, Chapel Hill, NC), respectively. Cuticle preparations were as in Wieschaus and Nüsslein-Volhard (1986).

Immunolocalization and immunoblotting

Embryos were bleach dechorionated and fixed for 20 min in 1:1 4% formaldehyde/0.1 M Pipes/2 mM $MgSO_4$/1 mM EGTA/0.1% NP-40:heptane. For DE-cadherin localization, embryos were fixed for 1 h in the same fix with 0.3% Triton X-100 added. Vitelline membranes were removed with methanol. For actin visualization, embryos were fixed for 5 min in 1:1 37% formaldehyde:heptane and their vitelline membranes were removed manually. Larval tissues were dissected in insect media and fixed in 4% paraformaldehyde in PBS for 20 min. Ovaries were dissected and fixed as in Peifer et al. (1993). All tissues were blocked and stained in PBS/1% goat serum/0.1% TritonX-100 (PBS/2% BSA/0.3% Triton X-100 was used for DE-cadherin staining). Antibodies used were mouse monoclonals antiphosphotyrosine (Upstate Biotechnology; 1:1,000), anti-Arm N27A1 (DSHB, 1:200), anti-Ena (1:500; Bashaw et al., 2000), BP102 (DSHB, 1:200), anti-Crumbs (DSHB; 1:2), anti-Coracle (9C and 16B, R. Fehon; 1:500 each), and anti-Neurotactin (DSHB; 1:5); rabbit polyclonals anti-Arm N2 (1:200) and anti-Ena (1:500) (Gertler et al., 1995); and rat monoclonals anti–α-catenin (1:250) (Oda et al., 1993) and anti–DE-cadherin (1:250) (Oda et al., 1994). Actin was visualized using Alexa 488 phalloidin (Molecular Probes). For DNA visualization, embryos were treated with 300 μg/ml RNase for 30 min at room temperature and stained for 20 min with 10 μg/ml propidium iodide. A ZEISS 410 laser scanning confocal microscope was used. For biochemical experiments, embryos were placed in halocarbon oil to allow staging under the dissecting microscope, picked at the cellular blastoderm stage, and aged defined periods of time. Extract preparation and cell fractionation were as in Peifer et al. (1993). Samples were analyzed by 6% SDS-PAGE, transferred to nitrocellulose and immunoblotted with mouse anti-Arm N27A1 (1:500), anti-Bicaudal D (B. Suter, McGill University, Montreal, Canada; 1:500), anti-pnut at (DSHB;1:30), antiactin (Chemicon; 1:250), rat anti–DE-cadherin1 (1:100), anti–α-catenin, anticoracle (both 1:500), and anticrumbs (1:50).

Time lapse microscopy

Wild-type embryos imaged were homozygous for Moesin-GFP (Kiehart et al., 2000), whereas *abl* mutant embryos imaged were derived from abl^4 germ line clone females crossed to abl^4, *FRT 79D-F*, moesin-GFP/*TM3* males; thus, the only GFP fluorescent embryos in this collection are those that are *abl* maternal/zygotic mutants. Embryos were bleach dechorionated and mounted in halocarbon oil (series 700; Halocarbon Products Corporation) between a coverslip and a gas permeable membrane (Petriperm; Sartorius Corporation). Images were captured every 30 s using a PerkinElmer Wallac Ultraview Confocal Imaging System, and image analysis was performed using NIH Image 1.62.

Online supplemental material

Time-lapse videos are available to supplement Fig. 5. Images were captured every 25 s and the videos are played at a rate of 10 frames/s. Videos are available at http://www.jcb.org/cgi/content/full/jcb.200105102/DC1.

We are grateful to E. Crafton and Z. Ozsoy for help with genetic interaction assays; to M. Hoffmann, G. Bashaw, R. Fehon, F. Fogerty, D. Kiehart, R. Saint, T. Uemura, U. Tepass, N. Brown, B. Suter, S. Crews, the Bloomington *Drosophila* Stock Center, and the Developmental Studies Hybridoma Bank for stocks or antibodies; to S. Whitfield for assistance with the figures; and to B. Duronio, B. McCartney, and the reviewers for helpful comments.

This work was supported by National Institutes of Health (NIH) grant R01 GM47857 to M. Peifer. E.E. Grevengoed was supported by NIH 5T32GM07092 and 1T32CA72319. T.L. Jesse was supported by NIH 5T3CA09156 and 1F32GM20797. M. Peifer was supported in part by the U.S. Army Breast Cancer Research Program.

Submitted: 22 May 2001
Revised: 5 November 2001
Accepted: 6 November 2001

References

Bashaw, G.J., T. Kidd, D. Murray, T. Pawson, and C.S. Goodman. 2000. Repulsive axon guidance: Abelson and Enabled play opposing roles downstream of the roundabout receptor. *Cell.* 101:703–715.

Baum, B., and N. Perrimon. 2001. Spatial control of the actin cytoskeleton in *Drosophila* epithelial cells. *Nat. Cell Biol.* 3:883–890.

Bear, J.E., J.J. Loureiro, I. Libova, R. Fassler, J. Wehland, and F.B. Gertler. 2000. Negative regulation of fibroblast motility by Ena/VASP proteins. *Cell.* 101: 717–728.

Bennett, R.L., and F.M. Hoffmann. 1992. Increased levels of the *Drosophila* Abelson tyrosine kinase in nerves and muscles: Subcellular localization and mutant phenotypes imply a role in cell-cell interactions. *Development.* 116:953–966.

Brown, N.H., S.L. Gregory, and M.D. Martin-Bermudo. 2000. Integrins as mediators of morphogenesis in *Drosophila*. *Dev. Biol.* 223:1–16.

Chou, T.B., and N. Perrimon. 1996. The autosomal FLP-DFS technique for generating germline mosaics in *Drosophila* melanogaster. *Genetics.* 144:1673–1679.

Comer, A.R., S.M. Ahern-Djamali, J.-L. Juang, P.D. Jackson, and F.M. Hoffmann. 1998. Phosphorylation of Enabled by the *Drosophila* Abelson tyrosine kinase regulates the in vivo function and protein-protein interactions of Enabled. *Mol. Cell. Biol.* 18:152–160.

Cox, R.T., C. Kirkpatrick, and M. Peifer. 1996. Armadillo is required for adherens junction assembly, cell polarity, and morphogenesis during *Drosophila* embryogenesis. *J. Cell Biol.* 134:133–148.

Daniel, J.M., and A.B. Reynolds. 1997. Tyrosine phosphorylation and cadherin/catenin function. *Bioessays.* 19:883–891.

Gertler, F., R. Bennett, M. Clark, and F. Hoffmann. 1989. *Drosophila* abl tyrosine kinase in embryonic CNS axons: a role in axonogenesis is revealed through dosage-sensitive interactions with disabled. *Cell.* 58:103–113.

Gertler, F., J. Doctor, and F. Hoffman. 1990. Genetic suppression of mutations in the *Drosophila abl* proto-oncogene homolog. *Science.* 248:857–860.

Gertler, F.B., A.R. Comer, J. Juang, S.M. Ahern, M.J. Clark, E.C. Liebl, and F.M.

Hoffmann. 1995. *enabled*, a dosage-sensitive suppressor of mutations in the *Drosophila* Abl tyrosine kinase, encodes an Abl substrate with SH3 domain-binding properties. *Genes Dev.* 9:521–533.

Gertler, F.B., K. Niebuhr, M. Reinhard, J. Wehland, and P. Soriano. 1996. Mena, a relative of VASP and *Drosophila* Enabled, is implicated in the control of microfilament dynamics. *Cell.* 87:227–239.

Henkemeyer, M., F. Gertler, W. Goodman, and F. Hoffmann. 1987. The *Drosophila* Abelson proto-oncogene homolog: identification of mutant alleles that have pleiotropic effects late in development. *Cell.* 51:821–828.

Henkemeyer, M., S. West, F. Gertler, and F. Hoffmann. 1990. A novel tyrosine kinase-independent function of *Drosophila* abl correlates with proper subcellular localization. *Cell.* 63:949–960.

Hirano, S., N. Kimoto, Y. Shimoyama, S. Hirohashi, and M. Takeichi. 1992. Identification of a neural α-catenin as a key regulator of cadherin function and multicellular organization. *Cell.* 70:293–301.

Iwai, Y., T. Usui, S. Hirano, R. Steward, M. Takeichi, and T. Uemura. 1997. Axon patterning requires DN-Cadherin, a novel neuronal adhesion receptor, in the *Drosophila* embryonic CNS. *Neuron.* 19:77–89.

Jacinto, A., W. Wood, T. Balayo, M. Turmaine, A. Martinez-Arias, and P. Martin. 2000. Dynamic actin-based epithelial adhesion and cell matching during *Drosophila* dorsal closure. *Curr. Biol.* 10:1420–1426.

Kiehart, D.P., C.G. Galbraith, K.A. Edwards, W.L. Rickoll, and R.A. Montague. 2000. Multiple forces contribute to cell sheet morphogenesis for dorsal closure in *Drosophila*. *J. Cell Biol.* 149:471–490.

Koleske, A.J., A.M. Gifford, M.L. Scott, M. Nee, R.T. Bronson, K.A. Miczek, and D. Baltimore. 1998. Essential roles for the Abl and Arg tyrosine kinases in neurulation. *Neuron.* 21:1259–1272.

Lanier, L.M., and F.B. Gertler. 2000. From Abl to actin: Abl tyrosine kinase and associated proteins in growth cone motility. *Curr. Opin. Neurobiol.* 10:80–87.

Lewis, J.M., R. Baskaran, S. Taagepera, M.A. Schwartz, and J.Y. Wang. 1996. Integrin regulation of c-Abl tyrosine kinase activity and cytoplasmic-nuclear transport. *Proc. Nat. Acad. Sci. USA.* 93:15174–15179.

Loureiro, J., and M. Peifer. 1998. Roles of Armadillo, a *Drosophila* catenin, during central nervous system development. *Curr. Biol.* 8:622–632.

Mauro, M.J., and B.J. Druker. 2001. Chronic myelogenous leukemia. *Curr. Opin. Oncol.* 13:3–7.

McEwen, D.G., R.T. Cox, and M. Peifer. 2000. The canonical Wg and JNK signaling cascades collaborate to promote both dorsal closure and ventral patterning. *Development.* 127:3607–3617.

Oda, H., T. Uemura, Y. Harada, Y. Iwai, and M. Takeichi. 1994. A *Drosophila* homolog of cadherin associated with Armadillo and essential for embryonic cell-cell adhesion. *Dev. Biol.* 165:716–726.

Oda, H., T. Uemura, K. Shiomi, A. Nagafuchi, S. Tsukita, and M. Takeichi. 1993. Identification of a *Drosophila* homologue of α-catenin and its association with *armadillo* protein. *J. Cell Biol.* 121:1133–1140.

Peifer, M., S. Orsulic, D. Sweeton, and E. Wieschaus. 1993. A role for the *Drosophila* segment polarity gene *armadillo* in cell adhesion and cytoskeletal integrity during oogenesis. *Development.* 118:1191–1207.

Quinlan, M.P., and J.L. Hyatt. 1999. Establishment of the circumferential actin filament network is a prerequisite for localization of the cadherin-catenin complex in epithelial cells. *Cell Growth Differ.* 10:839–854.

Stark, K.A., G.H. Yee, C.E. Roote, E.L. Williams, S. Zusman, and R.O. Hynes. 1997. A novel alpha integrin subunit associates with betaPS and functions in tissue morphogenesis and movement during *Drosophila* development. *Development.* 124:4583–4594.

Tepass, U., E. Gruszynski-DeFeo, T.A. Haag, L. Omatyar, T. Török, and V. Hartenstein. 1996. *shotgun* encodes *Drosophila* E-cadherin and is preferentially required during cell rearrangement in the neurectoderm and other morphogenetically active epithelia. *Genes Dev.* 10:672–685.

Tepass, U., K. Truong, D. Godt, M. Ikura, and M. Peifer. 2000. Cadherins in embryonic and neural morphogenesis. *Nat. Rev. Mol. Cell. Biol.* 1:91–100.

Uemura, T., H. Oda, R. Kraut, S. Hayashi, Y. Kotaoka, and M. Takeichi. 1996. Zygotic *Drosophila* E-cadherin expression is required for processes of dynamic epithelial cell rearrangement in the *Drosophila* embryo. *Genes Dev.* 10: 659–671.

Van Etten, R.A. 1999. Cycling, stressed-out and nervous: cellular functions of c-Abl. *Trends Cell Biol.* 9:179–186.

van Etten, R.A., P.K. Jackson, D. Baltimore, M.C. Sanders, P.T. Matsudeira, and P. Janmey. 1994. The COOH terminus of the c-Abl tyrosine kinase contains distinct F- and G-actin binding domains with bundling activity. *J. Cell Biol.* 124:325–340.

Vasioukhin, V., C. Bauer, M. Yin, and E. Fuchs. 2000. Directed actin polymerization is the driving force for epithelial cell-cell adhesion. *Cell.* 100:209–219.

Wieschaus, E., and C. Nüsslein-Volhard. 1986. Looking at embryos. *In Drosophila*, A Practical Approach. D.B. Roberts, editor. IRL Press, Oxford, England. 199–228.

Wills, Z., J. Bateman, C.A. Korey, A. Comer, and D. Van Vactor. 1999a. The tyrosine kinase Abl and its substrate enabled collaborate with the receptor phosphatase Dlar to control motor axon guidance. *Neuron.* 22:301–312.

Wills, Z., L. Marr, K. Zinn, C.S. Goodman, and D. Van Vactor. 1999b. Profilin and the Abl tyrosine kinase are required for motor axon outgrowth in the *Drosophila* embryo. *Neuron.* 22:291–299.

Young, P.E., A.M. Richman, A.S. Ketchum, and D.P. Kiehart. 1993. Morphogenesis in *Drosophila* requires nonmuscle myosin heavy chain function. *Genes Dev.* 7:29–41.

Zou, X., and K. Calame. 1999. Signaling pathways activated by oncogenic forms of Abl tyrosine kinase. *J. Biol. Chem.* 274:18141–18144.